JACS
JOURNAL OF THE AMERICAN CHEMICAL SOCIETY
Article
pubs.acs.org/JACS

Surface-Bound Molecular Rulers for Probing the Electrical Double Layer

Paul K. Eggers,[†] Nadim Darwish,[†] Michael N. Paddon-Row,* and J. Justin Gooding*

School of Chemistry, The University of New South Wales, Sydney, NSW, 2052, Australia

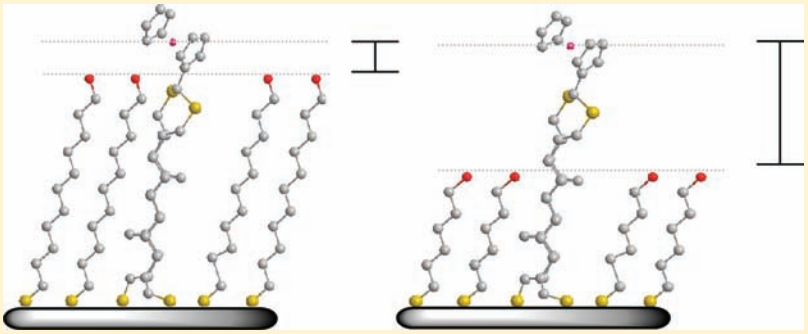

ABSTRACT: Herein, we report the first experimental investigation on the effect of varying the position of redox-active moieties, within the electrical double layer, on the apparent formal potential and on the electron transfer rate constant. This was achieved using a rigid class of molecules, norbornylogous bridges, to place redox species (ferrocene) at a fixed position above the surface of the electrode. Cyclic voltammetry and alternating current voltammetry were used to calculate the apparent formal potential and the electron transfer rate constant for the electron transfer between the ferrocene and the gold electrode. We use the effect of electric field on the apparent formal potential measurement of the surface-bound redox species to calculate the potential drop from the initiation of the electrical double layer to different distances above it. It was found that self-assembled monolayers formed from ω-hydroxyalkanethiol have a potential profile very similar to that described by classical theories for bare metal electrodes. A steep drop in potential in the Stern layer was observed followed by a smaller potential drop in the Gouy−Chapman layer. The electron transfer rate constant was found to decrease as the distance between the ferrocene moiety and the initiation of the double layer is increased. Thus, the electron transfer rate constant appears to be dependent on ion concentration.

INTRODUCTION

Within the electrical double layer is where electrochemical reactions take place. The electrical double layer polarizes species and concentrates ions of opposite charge on the electrode surface.[1] Theories on the structure of the electrical double layer date from the mid-1850s.[2] The most commonly used theory today, the Gouy−Chapman−Stern model, states that metal electrodes in contact with simple aqueous electrolytes form a region between the surface of the electrode and the locus of the first hydrated counterions, called the Stern layer, across which there is a linear drop in potential.[3] After the Stern layer is the diffuse layer, or the Gouy−Chapman layer,[3] which displays an approximately exponential decay in potential out to the bulk electrolyte according to the Poisson−Boltzmann equation.[2] If the metal electrode is modified by a self-assembled monolayer (SAM), another potential drop is added between the metal and the Stern layer.[4] Figure 1 shows the potential as a function of distance from the metal surface of an electrode modified with a SAM where the closest approach of ions in solution to the electrode is assumed to be the distal end of the SAM.

Although direct measurements of the surface charge and electrostatic potential for both bare electrodes and SAM-covered electrodes have been studied using atomic force microscopy technique,[5−7] the effect of the electrical double layer of a SAM-covered electrode on redox reactions is yet to be measured. The reason for this is the conformational flexibility of the commonly used alkanethiol SAM-forming molecules. The consequence of this flexibility is that it is not possible to unambiguously situate the redox centers at well-defined distances across the double layer.

Here, we demonstrate using rigid ferrocene-terminated norbornylogous bridges (Figure 2), the effect of the double layer on the electrochemical reaction, and present a new method to measure the potential drop across the electrical double layer. This method exploits the effect of electric field on the measurement of the formal potential of surface-bound redox species.[8]

The effect of the electric field on the formal potential that we exploit herein was first postulated by Smith and White,[4] as the theory of interfacial potential distribution, and was expanded to include the Stern layer by Fawcett.[9] In their seminal paper, Smith and White pointed out that the Nernst equation assumes that the potential difference between the surface of the electrode (whether it is the distal surface of a SAM or a

Received: February 26, 2012
Published: April 6, 2012

dx.doi.org/10.1021/ja301509h | J. Am. Chem. Soc. 2012, 134, 7539−7544

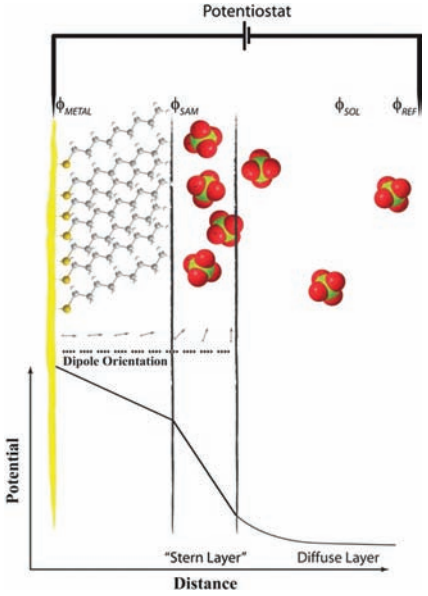

Figure 1. Cartoon of the electrical double layer.

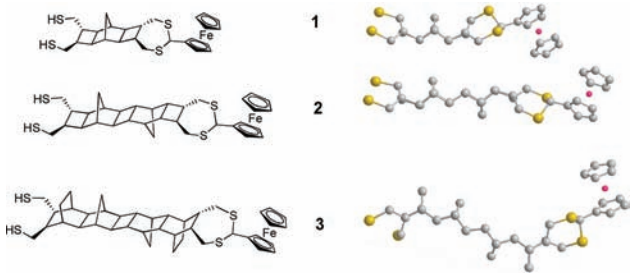

Figure 2. Structures of the molecules used in this study along with their BL3YP/6-31G(d) optimized structures. The ferrocenyl and thiol groups in compounds **1**–**3** are connected by chains comprising 10 σ, 13 σ, and 15 σ bonds, respectively.

metal surface) and the bulk solution is zero. This is, of course, not the case. The electric field created by a charged surface at the solid–electrolyte interface can not instantly become zero. Hence, an electrical double layer must form to balance the surface charge. We will review the derivation of Smith and White, as it was also central to the approach of Fawcett[9] and the approach adopted here. In an electrochemical system, the potential difference measured by a potentiostat is that between the bulk working electrode and the bulk reference electrode (the example used here is the silver, silver chloride reference half cell). This is described by the electrochemical cell in eq 1.

$$\mathrm{Au|O_s,\ R_s|Cl^-|AgCl|Ag} \tag{1}$$

Here, Au represents the bulk gold working electrode, which is modified with a low permittivity SAM, O_s and R_s are the oxidized and reduced forms of a surface-bound redox species, respectively, and $Cl^-|Ag|AgCl$ is the reference half cell. The stoichiometry of the electrochemical reaction (eq 2) implies an equilibrium of electrochemical potentials (eq 3).

$$\mathrm{O_s} + n\mathrm{Ag_s} + n\mathrm{Cl_l^-} + n\mathrm{e^-_{Au}} \rightleftarrows \mathrm{R_s} + n\mathrm{AgCl_s} + n\mathrm{e^-_{Ag}} \tag{2}$$

$$\bar{\mu}_{\mathrm{O}}^{\mathrm{PET}} + n\bar{\mu}_{\mathrm{Ag}}^{\mathrm{REF}} + n\bar{\mu}_{\mathrm{Cl^-}}^{\mathrm{SOL}} + n\bar{\mu}_{e^-}^{\mathrm{METAL}} = \bar{\mu}_{\mathrm{R}}^{\mathrm{PET}} + n\bar{\mu}_{\mathrm{AgCl}}^{\mathrm{REF}} + n\bar{\mu}_{e^-}^{\mathrm{REF}} \tag{3}$$

In eq 3, the superscripts refer to the location of the species, and the subscripts refer to the species. The four locations referred to in eq 3 are (1) the bulk working electrode (METAL); (2) the plane of electron transfer (PET), which is the spatial location of the redox species with respect to the surface of the working electrode; (3) the bulk solution (SOL), which is assumed to have no potential gradient; and (4) the reference electrode (REF). Equation 3 can be rewritten using standard thermodynamic definitions (including $\bar{\mu} = \mu^{\circ} + RT\ \ln[a] + zF\phi$) to form eq 4.

$$E = E^{\circ} + (\varphi_{\mathrm{PET}} - \varphi_{\mathrm{SOL}}) + \frac{RT}{nF}\ln\left[\frac{\Gamma_{\mathrm{O}}}{\Gamma_{\mathrm{R}}}\right] \tag{4}$$

Here, the measured potential difference is $E = (\phi_{\mathrm{METAL}} - \phi_{\mathrm{REF}})$. The term that is independent of surface coverage in eq 4 is not the formal potential, as in a classical Nernst formalism, but $E^{\circ} + (\phi_{\mathrm{PET}} - \phi_{\mathrm{SOL}})$, which we refer to as the "apparent formal potential". Therefore, the differences that have been observed in apparent formal potentials among various electroactive SAMs can be attributed to changes in $\phi_{\mathrm{PET}} - \phi_{\mathrm{SOL}}$ as the distal surface of the diluent interacts with the solution.[8] Furthermore, the potential drop across the Stern layer can be obtained from measurements of the apparent formal potential of modified electrodes, which are constructed with each PET at a different distance from the distal surface of the SAM. As the PET becomes further away from the distal end of the SAM $\phi_{\mathrm{PET}} - \phi_{\mathrm{SOL}}$ and hence the apparent formal potential, $E^{\circ} + (\phi_{\mathrm{PET}} - \phi_{\mathrm{SOL}})$, will decrease by the drop in potential of the Stern layer between the two points ($\phi_{\mathrm{SAM}} - \phi_{\mathrm{PET}}$ in Figure 3).

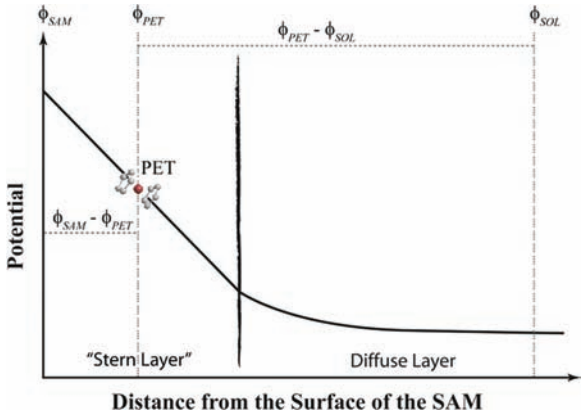

Figure 3. Schematic drawing describing the potential drop across the electrical double layer. ϕ_{SAM}, ϕ_{PET}, and ϕ_{SOL} are the potentials of the SAM (surface of the diluent), the plane of electron transfer, and the bulk solution, respectively.

The cause of the interfacial potential distribution, which is being described herein, is not the same as Smith and White described in their 1992 paper.[4] In that paper, they focused on the effects due to the oxidation of a neutral species to a positive ion without an ion pair. The charge of this newly created positive ion was then added to the surface charge, which in turn increased the potential difference between the surface of the SAM and the bulk solution. This, of course, assumes that there is no ion pairing. It can be seen from the equations of Calvente et al.[10] (who expanded the equations of Smith and White to include ion pairing) that if there is a very high degree of ion pairing, the increase in the potential difference, which was due to a charged oxidized species, is virtually nullified. It is known

dx.doi.org/10.1021/ja301509h | J. Am. Chem. Soc. 2012, 134, 7539–7544

that the ferrocene redox couple used herein forms a tight binding pair with the perchlorate ion.[11−14] Because the ferrocene forms an ion pair with the perchlorate ion at, or during, oxidation, the charge of the ferricinium is neutralized and does not need to be added to the charge at the surface of the monolayer. Thus, the effects being used herein to measure the potential drop across the double layer are those theorized by Fawcett[9] and shown to exist in a latter paper.[8]

This paper presents a method, which may be refined into a general technique, to probe the effects of the surface created by the terminal groups of a diluent on the electrostatic field near a modified electrode and how that field decays into the bulk solution. The keys to achieving this are the ferrocene-terminated norbornylogous bridges in Figure 2. We have previously characterized how these,[15] and related molecules,[16−18] assemble on a surface in mixed layers with conventional alkanethiols. We have shown in mixed SAMs that the norbornylogous bridges homogeneously distribute throughout the SAM, rather than cluster,[15] that they sit at an angle approximately 30° to the surface normal,[17−19] and that the orientation of the ferrocene moiety does not change on oxidation or reduction.[15] The purpose of this paper is to use these well-characterized molecules to explore electrical properties of an electrical double layer and their impact on electron transfer behavior. This is achieved by measuring the standard electron transfer rate constant and the apparent formal potential, $E^{o} + (\phi_{PET} - \phi_{SOL})$, at 0.11 nm increments away from the distal surface of the SAM under high ionic strength conditions. To demonstrate that this is a general technique, that is, independent of SAM thickness, two different series of constructs were tested.

RESULTS AND DISCUSSION

Construct Design. The method that we employed for probing the electrical and physical characteristics of the double layer uses a series of mixed monolayer constructs. Each construct places the ferrocene redox moiety at a well-defined height above the distal surface of the diluent. To compare each construct, the redox species used was kept the same, and the length of the diluent was changed. This allowed the coupling between the metal and the redox molecule to remain the same while varying the distance between the initiation of the double layer and the redox species using diluent of known thicknesses. This is illustrated by the five schematics in Figure 4. The distance between the center of the ferrocene moiety and the distal surface of the diluent was estimated based on the difference (Δ) between the height of the iron center from the gold surface and the height of each type of diluent taking into account a tilt of 30° from the surface normal for both the diluent[20] and the norbornylogous bridge[17] (see the Experimental Section for details). Three main criteria were used to ensure that the constructs used in this paper could provide the relevant data, namely: (1) The redox moiety is of sufficiently low coverage such that the double layer forms on the distal surface of the diluent and the redox moiety acts only as a probe of the double layer. (2) The redox moiety is fixed at a specific height above the distal surface of the diluent. (3) The electronic coupling pathways—which are responsible for mediating electron transfer between the ferrocene group and the gold electrode—should be confined to the norbornylogous bridge, with those taking a less direct route via adjacent diluent molecules playing a negligible role.

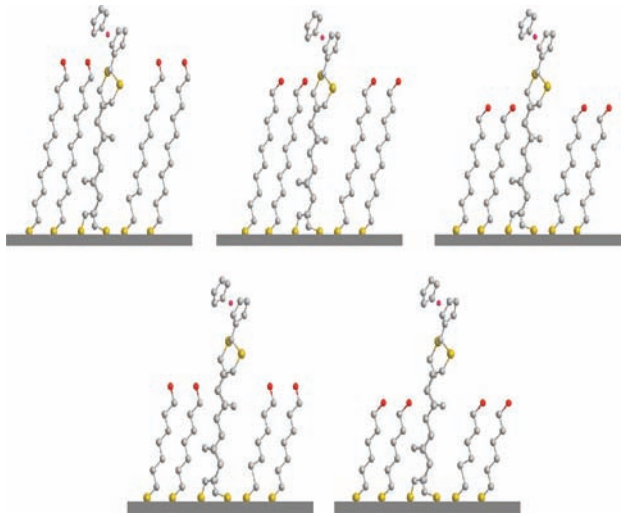

Figure 4. Sketch diagrams of the SAMs formed from compound **2** mixed with 11-mercaptoundecanol (**2**-11OH), compound **2** mixed with 10-mercaptodecanol (**2**-10OH), compound **2** mixed with 8-mercaptooctanol (**2**-8OH), compound **2** mixed with 7-mercaptoheptanol (**2**-7OH), and compound **2** mixed with 6-mercaptohexanol (**2**-6OH).

The first criterion ensures that the environment created by the double layer surrounding the ferrocene is measured and not an artifact created by other ferrocene redox moieties. This is addressed by using a very low surface coverage of the redox molecules. The coverages used in this paper were calculated from the area under the Faradaic waves of the CV for each construct and was between 17 and 39 nm^2 per redox-active molecule. The ferrocene moiety itself occupies an area of 0.29 nm^2; hence, the surface coverages of the ferrocene species protruding from the diluent is analogous to a pin sticking out of a cushion or between 0.74 and 1.7% of the electrode surface area. Scanning tunnelling microscopy images have been published previously, which demonstrate that the SAM formation technique used here gives an even dispersion of the ferrocene molecules without aggregation.[16] Thus, the ferrocene species will probe the electromagnetic field created by the double layer and not the electromagnetic field induced by other ferrocene moieties.

The second criterion underscores the need to have knowledge of the distance between the distal surface of the monolayer and the ferrocene. We have addressed this with previous studies. These norbornylogous bridges are rigid and hold their terminal groups above the distal surface of the SAM,[16,17,19] they have a ∼30 degree tilt angle which is similar to that found in alkanethiol SAMs,[17,19] the electrochemistry of the diluted SAMs formed by these norbornylogous bridges and alkanethiols (shown in Figure 5) is close to ideal with anodic−cathodic peak separation of less than 4 mV and full width half heights between 100 mV and 115 mV, they have no observable defects[16] and in diluted SAMs neither the tilt angle of the norbornylogous bridge or the diluent changes on oxidation or reduction of the ferrocene.[15,21] This last point means that the ferrocene is at the same position relative to the surface of the diluent throughout its oxidation and reduction. Hence these bridges fix the ferrocene at a specific height when they are mixed with a diluent to form a SAM and this height will remain constant throughout the electrochemical measurement.

The third criterion requires the ET process to occur exclusively through the NB bridge, without modulation by the alkyl chains of neighboring diluent molecules. Satisfying this requirement simplifies the interpretation of the ET rate data in

dx.doi.org/10.1021/ja301509h | J. Am. Chem. Soc. 2012, 134, 7539−7544

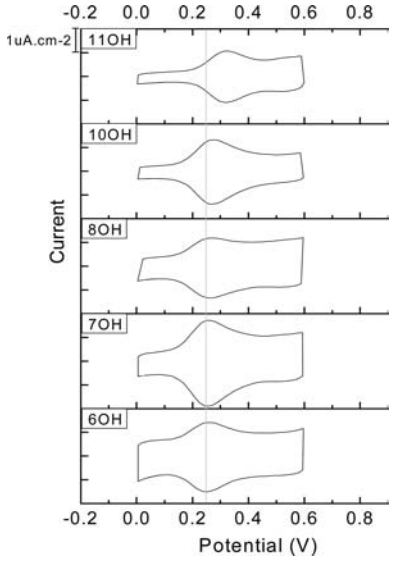

Figure 5. CVs at 100 mV/s of the mixed SAMs **2**-11OH, **2**-10OH, **2**-8OH, **2**-7OH, and **2**-6OH.

terms of the effects of the electrical double layer alone. A quantum chemical analysis of through-bond electronic coupling through hydrocarbon bridges led to the proposition that the coupling through a bridge could be enhanced by constructive interference with external coupling pathways supplied by alkyl chains, such as diluent molecules in mixed SAMs.[22] The presence of such enhanced coupling should result in a smaller value of the distance attenuation factor, β, which is obtained from the slope of the plot of $\ln(k_{et})$ vs bridge length. Thus, diluent-enhanced coupling in our NB systems is expected to give a β value significantly smaller than the normal β values of 0.92−1.25 bond^{-1}, obtained for NB bridges in solution.[22−24] Figure 6 shows the plot derived from the rate constant

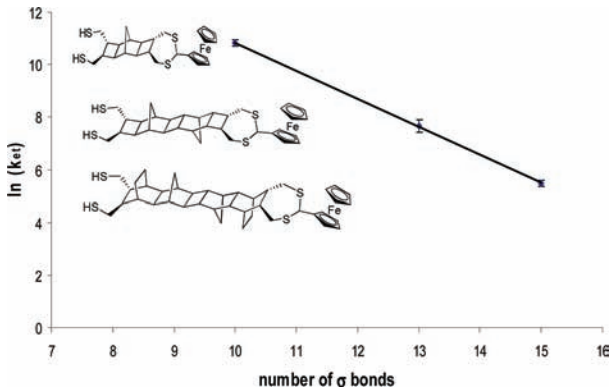

Figure 6. Electron transfer−bridge length plot for SAMs composed of compound **1** mixed with 4-mercaptobutanol (**1**-4OH), compound **2** mixed with 7-mercaptoheptanol (**2**-7OH), and compound **3** mixed with 8-mercaptooctanol (**3**-8OH). The plot has a slope of −1.1 and an R^2 = 0.9997. In all three SAMs, the distance between the ferrocene moiety and the surface of the diluent was held constant (estimated to be 0.7 nm); therefore, the environment around the ferrocene redox center in all three SAMs is comparable. β = 1.1 bond^{-1}.

measured for molecules **1**−**3**, which possess 10, 13, and 15 σ bonds, respectively. To maintain a similar environment around the ferrocene moiety, compound **1** was mixed with 4-mercaptobutanol (4OH) diluent, compound **2** with 7-mercaptoheptanol (7OH) diluent, and compound **3** with 8-mercaptooctanol (8OH) diluent. That is, the distance between the center of the ferrocene moiety and the surface of the diluent in all three SAMs was the same and was ca. 0.7 nm. From the slope of the plot (Figure 6), a β value of 1.1 bond^{-1} is obtained. The fact that the β-value is similar and not smaller than that observed in solution signifies that the diluent molecules are not significantly influencing the electron transfer rates in our SAMs.

Measurement of the Potential Drop across the electrical double layer. To situate the ferrocene moiety at a well-defined position above the distal surface of the diluent, compounds **1** and **2** were used as they are linear in contrast to **3** that has a slight curvature in its backbone (Compound **3** has a slight curvature in its backbone, which can induce less-ordered SAMs in the case where diluent of comparable length to compound **3** is used. Evidence of disordered SAMs came from the observation of multiple peaks in the CVs when diluent of comparable length to compound **3** was used.) (confirmed by BL3YP/6-31G(d) calculations; see Figure 2). It can be seen from Figure 7 that the potential drops for the equivalent

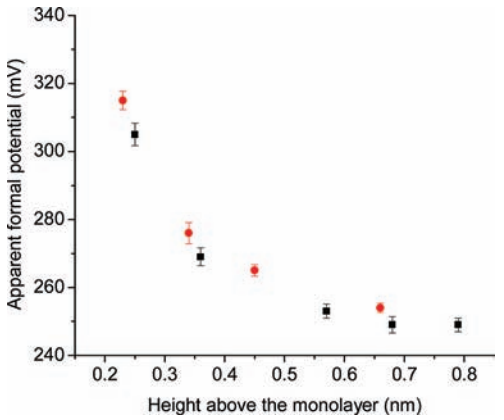

Figure 7. Overlay of the plots of the apparent formal potential vs the distance between the ferrocene moiety of compounds **1** (red circles) and **2** (black squares) and the distal surface of the diluent. The potential drops for the equivalent constructs of compounds **1** and **2** match closely.

constructs of compounds **1** and **2** match very closely. This validates the capacity of these constructs to elucidate a similar $\phi_{PET} - \phi_{SOL}$ irrespective of the length of the norbornylogous bridge used. In the data sets for constructs of both compounds **1** and **2**, there was a steep drop in potential from the distal surface of the diluent to at least 0.45 nm above it. This is followed by a very small potential drop between 0.5 and 0.8 nm. The steep drop approximately corresponds to the diameter of a perchlorate ion, 0.47 nm.[11] Hence, we propose that the initial drop is created by a layer of perchlorate ions, which, according to the model of a double layer on a bare metal electrode, would be classified as the Stern layer. This suggests that the small potential drop between 0.5 and 0.8 nm corresponds to the Gouy−Chapman layer. The distances in Figure 7 correlate with a simple calculation of the thickness of the double layer by adding the thickness of the Stern layer to the Debye length, κ^{-1} (thickness of the Gouy−Chapman layer), as calculated via eq 5

$$\kappa^{-1} = \sqrt{\frac{\varepsilon_0 \varepsilon_r kT}{2N_A e^2 cz^2}} \quad (5)$$

dx.doi.org/10.1021/ja301509h | J. Am. Chem. Soc. 2012, 134, 7539−7544

where ε_0 is the permittivity of the vacuum, ε_r is the dielectric constant, k is the Boltzmann constant, T is the temperature in Kelvin (K), N_A is the Avogadro number, e is the elementary charge, c is the concentration of the electrolyte in moles m^{-3}, and z is the charge number.[2] For an electrolyte concentration of 1 M $HClO_4$ used here, eq 5 gives a Debye length of 0.3 nm. Given the Stern layer can be roughly defined as the diameter of the counterion, a 0.47 nm perchlorate ion in this case, the combined thickness of the Stern layer and Gouy−Chapman layer should equate to approximately 0.77 nm. Thus, according to eq 4 and the data in Figure 7, 249 mV is either the formal potential or very close to the formal potential of compounds **1** and **2**.

Rates of Electron Transfer Relative to the Position of the Ferrocene. The same constructs presented in Figure 4 were used to calculate the electron transfer rate constant of the electron transfer between the ferrocene and the gold electrode. It can be seen from Figure 8 that the standard electron transfer rate constant, calculated using the alternating current voltammetry technique,[25] decreases with an increase in the distance between the ferrocene and the surface of the diluent. As shown in Figures 1 and 7, the electrostatic field strength also follows the same trend, thereby lending ambiguity as to the actual cause of the decrease in the rate constant. However, the apparent formal potential does not relate to an increase in the reaction's overpotential, but the activation energy of the reaction and, hence, would have a minimal effect on the rate constant. Therefore, we conclude that the leading cause of the decrease in rate of electron transfer is, most likely, the decrease in ion concentration. This conclusion is supported by the ferrocene redox reactions being highly dependent on ion availability.[1] It can be envisioned that the monolayer of perchlorate ions (our proposed Stern layer) will interact with the positive charge on the electrode. Thus, in the Stern layer, the perchlorate ions are more readily available to bind with the ferricinium cations as compared with the perchlorate ions in the bulk solution. As a consequence, as the ferrocene moiety is progressively situated away from the distal surface of the diluent, the rate constant for electron transfer decreases.

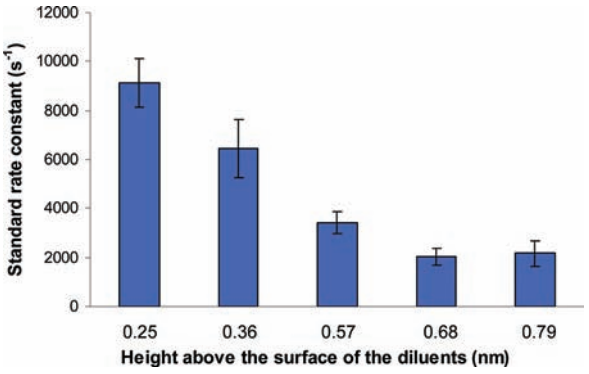

Figure 8. Variation of the electron transfer rate constant with varying distance between the ferrocene moiety and the surface of the diluent. Each bar represents the rate constant calculated for the SAMs constructed from compound **2** mixed with 11-mercaptoundecanol (**2**-11OH, 0.25 nm), compound **2** mixed with 10-mercaptoundecanol (**2**-10OH, 0.36 nm), compound **2** mixed with 8-mercaptooctanol (**2**-8OH, 0.57 nm), compound **2** mixed with 7-mercaptoheptanol (**2**-7OH, 0.68 nm), and compound **2** mixed with 6-mercaptohexanol (**2**-6OH, 0.79 nm).

The ferrocene redox species is ideal for demonstrating that it is possible to use the technique presented herein to measure the potential drop across the Stern layer and into the diffuse layer. For instance, the separation of the anodic and cathodic peaks in the CVs of these ferrocene derivatives is close to zero and thus gives accurate values for apparent formal potentials. Furthermore, the Faradaic current is ideally situated at potentials where the monolayers of ω-hydroxyalkanethiol are known to be ionic blocking[21,26] and the diluent does not change its tilt angle.[15,21] Hence, ferrocene has enabled us to show for the first time that the potential drop across the electrical double layer can be mapped in 0.11 nm steps above the surface, allowing us to get three data points across the diameter of a perchlorate ion with high confidence on the apparent formal potentials. From this, we showed that within the Faradaic window of compounds **1** and **2**, the monolayers of ω-hydroxyalkanethiol have a similar double layer structure to what a bare metal electrode was predicted to have. The results demonstrate that this technique allows the potential profile of the electrical double layer to be measured and that that potential profile agrees with theory.

CONCLUSION

This paper has presented a method for measuring the potential in a double layer at 0.11 nm steps above the surface of a modified electrode. It has shown that for SAMs formed from ω-hydroxyalkanethiol, the Stern layer appears to be made up of a monolayer of perchlorate ions and has a potential profile very similar to that proposed for a bare metal electrode. It has shown that the electron transfer rate constant decays with the distance from the surface and thus appears to be dependent on ion concentration.

EXPERIMENTAL SECTION

Materials. The ferrocene-derived norbornylogous bridges were synthesized as outlined in previous papers.[16,17] 4-Mercaptobutanol (4OH), 6-mercaptohexanol (6OH), and 11-mercaptoundecanol (11OH) were purchased from Sigma Aldrich (>98%). 7-Mercaptoheptanol (7OH), 8-mercaptooctanol (8OH), and 10-mercatodecanol (10OH) were synthesized according to standard procedures.[8]

Preparation of Au (111) Single Gold Crystals Electrodes. Au (111)-exposed single-crystal substrates were prepared by melting the ends of Au wire (0.5 mm in diameter; Goodfellow) according to the method of Clavilier et al.[27] and Hamelin.[28] The mechanically exposed Au (111) single-crystal surfaces were used for all of the electrochemical measurements. The quality of the electrodes was checked by recording the cyclic voltammograms (CVs) of the electrodes in 0.1 M H_2SO_4, which was found to be consistent with reported CVs, and by scanning tunneling microscopy (STM). The detailed experimental procedure for fabricating the surfaces used in this study is published elsewhere.[29]

Surface Modification. The mixed monolayers were prepared using redistilled dichloromethane (DCM) solutions of the NB mixed with ω-hydroxyalkanethiol in a ratio 1 to 50, respectively. The total concentration of the mixed monolayer was 1 mM. Freshly annealed Au (111) gold single crystals were immersed in the mixed solution for 10 min. The crystals were then rinsed thoroughly with DCM before immersing in a DCM solution with a 1 mM concentration of the ω-hydroxyalkanethiol as the only component over a period of 24 h. Prior to the electrochemical measurements, the crystals were rinsed with DCM, ethanol, and Milli-Q water.

Distance between the Ferrocene Center and the Surface of the Diluent. Table 1 presents the distances between the iron center of the ferrocene moiety and the distal groups of the diluent in each SAM. The distances were estimated by the difference (Δ) between the height of the iron center from the gold surface and the height of each

dx.doi.org/10.1021/ja301509h | J. Am. Chem. Soc. 2012, 134, 7539−7544

Table 1. Distances between the Iron Center of the Ferrocene Moiety and the Distal Groups of the Diluent in Each SAM

diluent	length (nm)	Δ distance (nm)
11OH	1.38	**2**-11OH = 0.25
10OH	1.27	**2**-10OH = 0.36
8OH	1.06	**2**-8OH = 0.57
		1-8OH = 0.23
7OH	0.95	**2**-7OH = 0.68
		1-7OH = 0.34
6OH	0.84	**2**-6OH = 0.79
		1-6OH = 0.45
4OH	0.63	**1**-4OH = 0.66

type of diluent, taking into account a tilt of 30° from the surface normal. The distance between the ferrocene center and the gold surface was estimated using the known length of the molecules (according to the BL3YP/6-31G(d) optimized structure of the molecules), taking into account the 30° tilt of the NB molecules on the gold surface.[17,19] The distance from the iron center to the gold surface was 1.29 and 1.63 nm for molecules **1** and **2**, respectively.

Cyclic Voltammetry. Cyclic voltammetry experiments were performed using a three-electrode cell containing a gold single-crystal (111) working electrode by forming a meniscus with the electrolyte, a platinum mesh counter electrode, and a 3 M NaCl Ag/AgCl reference electrode in a 1 M perchloric acid (Merck) serving as an electrolyte. The counter electrode was placed parallel to the working electrodes surface. Contact with the working electrode was made via a platinum wire. The CVs were recorded using a Solartron 1287 Electrochemical Interface. The separation of oxidation and reduction peaks of the CVs used herein was all less than 4 mV. This resulted in an uncertainty for the apparent formal potential of less than 2 mV.

AC Voltammetry. AC voltammetry was performed using a three-electrode cell containing a gold single-crystal (111) working electrode, a platinum foil counter electrode, and a AglAgCl 3 M NaCl reference electrode. The AC voltammograms (ACVs) were collected using a Solartron 1287 Electrochemical Interface with a 1260 Solartron Impedance/Gain-Phase Analyzer. The calculation of the rate constant of electron transfer was conducted using a program written in Matlab according to the method outlined by Creager et al.[25] Measurement uncertainties of rate constants are dominated by the signal-to-noise ratios of currents, which are a consequence of the small surface coverage of the redox moieties. To minimize this uncertainty, the same fitting parameters for peak baselines were used for each series of constructs.

AUTHOR INFORMATION

Corresponding Author

*E-mail: m.paddonrow@unsw.edu.au; Justin.gooding@unsw.edu.au

Author Contributions

†These authors contributed equally.

Notes

The authors declare no competing financial interest.

ACKNOWLEDGMENTS

The Australian research council is acknowledged for funding.

REFERENCES

(1) Sumner, J. J.; Creager, S. E. *J. Phys. Chem. B* **2001**, *105*, 8739−8745.

(2) Bard, A. J.; Faulkner, L. R. *Electrochemical Methods: Fundamentals and Applications*, 2nd ed.; John Wiley & Sons: New York, 2001.

(3) Delgado, A. V.; Gonzalez-Caballero, F.; Hunter, R. J.; Koopal, L. K.; Lyklema, J. *Pure Appl. Chem.* **2005**, *77*, 1753−1805.

(4) Smith, C. P.; White, H. S. *Anal. Chem.* **1992**, *64*, 2398−2405.

(5) Hu, K.; Chai, Z.; Whitesell, J. K.; Bard, A. J. *Langmuir* **1999**, *15*, 3343−3347.

(6) Kane, V.; Mulvaney, P. *Langmuir* **1998**, *14*, 3303−3311.

(7) Rentsch, S.; Siegenthaler, H.; Papastavrou, G. *Langmuir* **2007**, *23*, 9083−9091.

(8) Eggers, P. K.; Hibbert, D. B.; Paddon-Row, M. N.; Gooding, J. J. *J. Phys. Chem. C* **2009**, *113*, 8964−8971.

(9) Fawcett, W. R. *J. Electroanal. Chem.* **1994**, *378*, 117.

(10) Calvente, J. J.; Andreu, R.; Molero, M.; Lopez-Perez, G.; Dominguez, M. *J. Phys. Chem. B* **2001**, *105*, 9557−9568.

(11) Rowe, G. K.; Creager, S. E. *J. Phys. Chem.* **1994**, *98*, 5500−5507.

(12) Creager, S. E.; Rowe, G. K. *Anal. Chim. Acta* **1991**, *246*, 233−239.

(13) Yao, X.; Wang, J.; Zhou, F.; Wang, J.; Tao, N. *J. Phys. Chem. B* **2004**, *108*, 7206−7212.

(14) Redepenning, J.; Castro-Narro, E.; Venkataraman, G.; Mechalke, E. *J. Electroanal. Chem.* **2001**, *498*, 192−200.

(15) Eggers, P. K.; Da Silva, P.; Darwish, N. A.; Zhang, Y.; Tong, Y.; Ye, S.; Paddon-Row, M. N.; Gooding, J. J. *Langmuir* **2010**, *26*, 15665−15670.

(16) Eggers, P. K.; Zareie, H. M.; Paddon-Row, M. N.; Gooding, J. J. *Langmuir* **2009**, *25*, 11090−11096.

(17) Yang, W. R.; Jones, M. W.; Li, X.; Eggers, P. K.; Tao, N.; Gooding, J. J.; Paddon-Row, M. N. *J. Phys. Chem. C* **2008**, *112*, 9072−9080.

(18) Darwish, N.; Eggers, P. K.; Da Silva, P.; Zhang, Y.; Tong, Y.; Ye, S.; Gooding, J. J.; Paddon-Row, M. N. *Chem.—Eur. J.* **2012**, *18*, 283−292.

(19) Beebe, J. M.; Engelkes, V. B.; Liu, J.; Gooding, J. J.; Eggers, P. K.; Jun, Y.; Zhu, X.; Paddon-Row, M. N.; Frisbie, C. D. *J. Phys. Chem. B* **2005**, *109*, 5207−5215.

(20) Cossaro, A.; Mazzarello, R.; Rousseau, R.; Casalis, L.; Verdini, A.; Kohlmeyer, A.; Floreano, L.; Scandolo, S.; Morgante, A.; Klein, M. L.; Scoles, G. *Science* **2008**, *321*, 943−946.

(21) Darwish, N.; Eggers, P. K.; Ciampi, S.; Zhang, Y.; Tong, Y.; Ye, S.; Paddon-Row, M. N.; Gooding, J. J. *Electrochem. Commun.* **2011**, *13*, 387−390.

(22) Paddon-Row, M. N.; Shephard, M. J. *J. Am. Chem. Soc.* **1997**, *119*, 5355−5365.

(23) Paddon-Row, M. N. *Acc. Chem. Res.* **1994**, *27*, 18−25.

(24) Seischab, M.; Lodenkemper, T.; Stockmann, A.; Schneider, S.; Koeberg, M.; Roest, M. R.; Verhoeven, J. W.; Lawson, J. M.; Paddon-Row, M. N. *Phys. Chem. Chem. Phys.* **2000**, *2*, 1889−1897.

(25) Creager, S. E.; Wooster, T. T. *Anal. Chem.* **1998**, *70*, 4257−4263.

(26) Boubour, E.; Lennox, R. B. *Langmuir* **2000**, *16*, 7464−7470.

(27) Clavilier, J.; Armand, D.; Wu, B. L. *J. Electroanal. Chem.* **1982**, *135*, 159−166.

(28) Hamelin, A. *J. Electroanal. Chem.* **1996**, *407*, 1−11.

(29) Darwish, N. A.; Eggers, P. K.; Yang, W.; Paddon-Row, M. N.; Gooding, J. J. Nanoscience and Nanotechnology (ICONN), 2010 International Conference, 22−26 Feb 2010, pp 302−305.